Biochemistry

 Volume 37, Number 21 May 26, 1998

*Accelerated Publications*

# Energetic Roles of Hydrogen Bonds at the Ureido Oxygen Binding Pocket in the Streptavidin−Biotin Complex†

Lisa A. Klumb,‡ Vano Chu, and Patrick S. Stayton*

*Department of Bioengineering, Box 357962, University of Washington, Seattle, Washington 98195*

*Received February 6, 1998; Revised Manuscript Received April 14, 1998*

ABSTRACT: The high-affinity streptavidin−biotin complex is characterized by an extensive hydrogen-bonding network. A study of hydrogen-bonding energetics at the ureido oxygen of biotin has been conducted with site-directed mutations at Asn 23, Ser 27, and Tyr 43. A new competitive biotin binding assay was developed to provide direct equilibrium measurements of the alterations in $K_d$. S27A, Y43F, Y43A, N23A, and N23E mutants display $\Delta\Delta G°$ at 37 °C relative to wild-type streptavidin of 2.9, 1.2, 2.6, 3.5, and 2.6 kcal/mol, respectively. The equilibrium-binding enthalpies for all of the mutants were measured by isothermal titration calorimetry, and the Y43A and N23A mutants display large decreases in the equilibrium binding enthalpy at 25 °C of 8.9 and 6.9 kcal/mol, respectively. The S27A and N23E mutants displayed small decreases in binding enthalpy of 1.6 and 0.9 kcal/mol relative to wild-type, while the Y43F mutant displayed a −2.6 kcal/mol increase in the binding enthalpy at 25 °C. At 37 °C, the Y43A and N23A mutants display decreases of 7.8 and 7.9 kcal/mol, respectively, while the S27A, N23E, and Y43F mutants displayed decreases of 4.9, 3.7, and 1.2 kcal/mol relative to wild-type. Kinetic analyses were also conducted to probe the contributions of the hydrogen bonds to the activation barrier. Wild-type streptavidin at 37 °C displays a $k_{off}$ of $(4.1 \pm 0.3) \times 10^{-5}$ s$^{-1}$, and the conservative Y43F, S27A, and N23A mutants displayed increases in $k_{off}$ to $(20 \pm 1) \times 10^{-5}$ s$^{-1}$, $(660 \pm 40) \times 10^{-5}$ s$^{-1}$, and $(1030 \pm 220) \times 10^{-5}$ s$^{-1}$, respectively. The Y43A and N23E mutants displayed 93-fold and 188-fold increases in $k_{off}$, respectively. Activation energies and enthalpies for each of the mutants were determined by transition-state analysis of the dissociation rate temperature dependence. All of the mutants except Y43F display large reductions in the activation enthalpy. The Y43F mutant has a more positive activation enthalpy, and thus a more favorable activation entropy that underlies the overall reduction in the activation barrier. For the most conservative mutant at each ureido oxygen hydrogen-bonding position, bound-state alterations account for most of the energetic changes in a single transition-state model, suggesting that the ureido oxygen hydrogen-bonding interactions are broken in the dissociation transition state.

The high-affinity streptavidin−biotin system provides a good model system for investigating the relationships between molecular structure and protein−ligand energetics. The X-ray crystal structures for streptavidin and avidin complexed with biotin (*1*−*5*) reveal three structural motifs common to other tight-binding protein−ligand systems: van

† This work was supported by Grant DK49655 from the National Institutes of Health.

* To whom correspondence should be addressed. Phone: (206) 685-8148. Fax: (206) 685-8256. E-mail: stayton@bioeng.washington.edu.

‡ Current Address: Pharmaceutics, Mail Stop 8-1-C, Amgen, One Amgen Center Drive, Thousand Oaks, CA 91320-1789.

S0006-2960(98)00312-2 CCC: $15.00 
Published on Web 05/08/1998

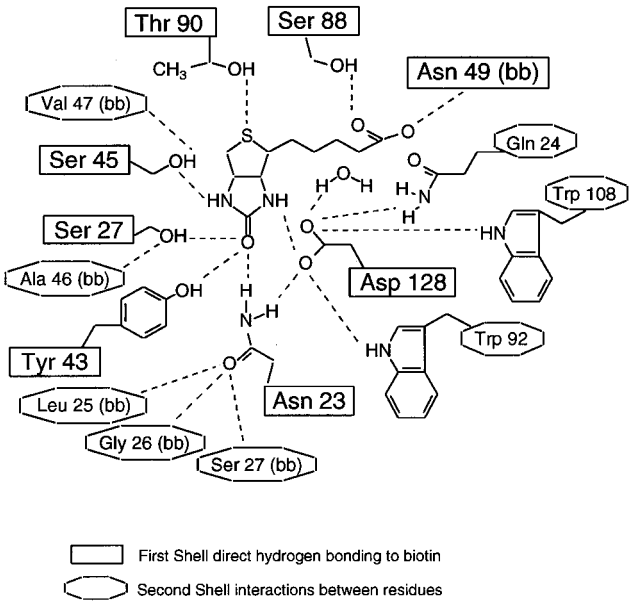


FIGURE 1: Schematic of the hydrogen-bonding network established between streptavidin and biotin as determined from the crystallographic structure of the bound protein−ligand complex (*1*, *24*). Direct hydrogen bonds between protein side chains and biotin are designated as first shell interactions. Second shell interactions are those between the protein backbone (denoted as "bb") or other side chains and the first shell protein side chains.

der Waals interactions including aromatic side-chain contacts (*6*−*10*); an extensive hydrogen-bonding network (*11*−*16*); and the ordering of surface peptide loops upon biotin binding (*17*−*19*). Because numerous protein−ligand interactions utilize these structural motifs, elucidation of the structure−function relationships underlying the slow streptavidin−biotin dissociation kinetics could provide generally useful insight into tight-binding protein−ligand interactions.

Experimental and computational studies have suggested that the hydrophobic and van der Waals interactions play an important role in generating the large binding free energy (*20*−*22*). The tryptophan residues in the binding site contribute the most prominent aromatic interactions, as was first postulated by Green (*23*). In addition to these tryptophan contacts, however, there is a prominent set of primary hydrogen-bonding interactions and associated network interactions that extend into the adjacent protein structure (Figure 1). Weber and co-workers have proposed that the ureido oxygen of biotin is unusually polarized in the complex, with the oxygen existing in an oxyanion resonance form (*24*). They hypothesized that the hydrogen-bonding network focuses complementary electrostatic interactions with this ureido oxyanion and that these interactions could thus make a relatively large free-energy contribution to streptavidin−biotin association.

We investigate here the energetic consequences of disrupting hydrogen bonding to the biotin ureido oxygen. Asn 23, Ser 27, and Tyr 43 form hydrogen bonds with the ureido oxygen of biotin, and all three residues are conserved in the avidin−biotin system. We present a site-directed mutagenesis study of these three residues with an analysis of the hydrogen-bonding contributions to the equilibrium binding free energy and enthalpy. This system has also provided an interesting opportunity to investigate hydrogen-bonding contributions to the activation thermodynamics, as the exceptionally tight binding is controlled by slow dissociation kinetics (*21*, *25*).

## MATERIALS AND METHODS

*Gene Construction, Protein Expression, and Purification.* The design and mutagenesis of the recombinant core streptavidin gene and the expression of all mutants in a T7 expression system (pET-21a, Novagen Inc., Madison, WI) were performed as reported previously (*20*). Briefly, all proteins were expressed as insoluble inclusion bodies, which were isolated and then dissolved in 6 M guanidine hydrochloride, followed by refolding via dilution into Tris buffer, pH 8.0. Refolded protein was purified by affinity chromatography with iminobiotin-agarose (Pierce, Rockford, IL). Protein concentrations were determined for the wild-type (WT) and the mutants using an extinction coefficient of 34 000 $M^{-1}$ $cm^{-1}$/subunit. Preliminary structural and functional characterization of the mutants included SDS and native PAGE, electrospray mass spectrometry, and biotin binding stoichiometry determination via titration with fluorescein-biotin (Molecular Probes, Eugene, OR).

*Determination of Binding Free-Energy Alterations.* An assay was developed to measure the thermodynamic free-energy alterations for the mutants relative to wild-type streptavidin. A "His tag" with six histidines added to the C-terminus of streptavidin was constructed, which allowed immobilization on Ni-NTA resin (Superflow, Qiagen). In a mixture of [$^3$H]biotin with the His tag streptavidin (WT-HisTag) and competing streptavidin, the partitioning of [$^3$H]-biotin between the two proteins at equilibrium can be determined after removal of the WT-HisTag via the Ni-NTA resin. A complete competition curve is generated by varying the concentration of the competing streptavidin, keeping the concentrations of the WT-HisTag and [$^3$H]biotin constant and determining the amount of [$^3$H]biotin bound to the competing streptavidin after equilibration. [$^3$H]Biotin (21 $\mu$M, Amersham, Chicago, IL) was added to a final concentration of 20 nM to mixtures of the WT-HisTag (50 nM) and competing streptavidin in phosphate buffered saline (50 mM $NaH_2PO_4$, 100 mM NaCl), pH 6.5−7.0. The concentration of the competing streptavidin was varied from 0 nM to 50 × $\Delta K_d$ × 50 nM, where $\Delta K_d$ is the ratio of the biotin equilibrium dissociation constants, competing streptavidin to WT-HisTag. Imidazole (20 mM) was added to minimize any nonspecific adsorption of the competing streptavidin due to the four native histidines. The solution containing the protein and ligand was equilibrated over several half-lives for the wild-type streptavidin−biotin dissociation rate ($t_{1/2}$ is 4.7 h at 37 °C) with typical incubation times of 24 h at 37 °C. After equilibration, the WT-HisTag streptavidin was removed by batch incubation for 1 h with 50 $\mu$L of a 50% slurry of washed Ni-NTA resin. The mixture was then cleared extensively via centrifugation. The supernatants were collected, heated at 90 °C in 5% SDS for 30 min to liberate bound [$^3$H]biotin, and assayed for radioactivity. Under these conditions, 98% of the WT-HisTag streptavidin was removed from solution by the Ni-NTA resin, and nonspecific binding of the competing streptavidin to the resin varied between 2 and 5%. A negligible amount of [$^3$H]biotin was found to bind to the Ni-NTA resin in the absence of streptavidin and in the presence of protein the free [$^3$H]biotin was less than 2% of the total ligand concentration.

The amount of [$^3$H]biotin bound to the competing streptavidin was plotted as a function of the total concentration of the competing streptavidin, with the WT-HisTag streptavidin and [$^3$H]biotin concentrations kept constant. The solution to the quadratic expression shown in eq 1 was applied to the data with the ratio of the dissociation constants ($\Delta K_d = K_C/K_P$) as a fitting parameter using nonlinear $\chi^2$ minimization (Igor Pro, Wavemetrics, Inc., Lake Oswego, OR):

$$\left(\frac{K_C}{K_P} - 1\right)[C - L]^2 + \left(L_T + C_T + \frac{K_C}{K_P}(P_T - L_T)\right)[C - L] - L_T C_T = 0 \quad (1)$$

where $K_C = [C][L]/[C - L]$ is the equilibrium dissociation constant for non-His tag streptavidin (competitor), $K_P = [P][L]/[P - L]$ is the equilibrium dissociation constant for the WT-HisTag streptavidin, [C] is the concentration of competing streptavidin, [P] is the concentration of WT-HisTag streptavidin, [L] is the concentration of ligand ([$^3$H]biotin), and $X_T$ is the total concentration of parameter $X$.

Equation 1 was derived from the ratio of the equilibrium dissociation constants of the WT and WT-HisTag streptavidin−biotin complexes, the mass balances for both streptavidins, and the [$^3$H]biotin using the assumption of negligible free [$^3$H]biotin which was verified in each experiment.

*Isothermal Titration Calorimetry.* The binding enthalpies at 25 and 37 °C were determined using isothermal titration calorimetry (ITC) as described previously (*21*) with the following modifications. A CSC 4200 titration calorimeter (Calorimetry Sciences Corporation, Provo, UT) was used for all of the experiments. Streptavidin solutions (33−38 $\mu$M in subunit concentration) were titrated with 15−20 injections of biotin (250 or 500 $\mu$M, 5−10 $\mu$L/injection), and the heat flow between the reaction vessel and an isothermal heat sink was monitored. The buffer system was 50 mM phosphate and 100 mM NaCl, pH 7. The data was analyzed with software developed for the CSC 4200 (Dataworks and Bindworks), by determining the observed reaction heat for each titration step. Nonlinear least-squares fitting of the corrected reaction heat allowed the binding stoichiometry ($n$) and equilibrium binding enthalpy ($\Delta H°$) to be determined, assuming no cooperativity between subunits of the tetrameric streptavidin.

*Streptavidin−Biotin Dissociation Kinetics.* The streptavidin−biotin dissociation kinetics were determined using a method modified from that described previously (*21*). 8,9-[$^3$H]Biotin (21 $\mu$M, Amersham) at a concentration of 10 nM was incubated for 20 min with 1 $\mu$M subunit concentration of streptavidin (WT or mutants). To initiate the dissociation reaction, nonradioactive biotin was added to a final concentration of 50 $\mu$M. The unbound biotin was separated from the protein−ligand complex at various times by either centrifugal ultrafiltration through a 30 000 MW cutoff filter (Microcon-30, Amicon Inc., Beverly, MA) or zinc sulfate precipitation of the protein−ligand complex (0.2 M zinc sulfate and 0.2 M NaOH). The nonspecific binding of [$^3$H]-biotin to the filter varied between 3 and 10%, whereas the zinc sulfate precipitated less than 5% of the [$^3$H]biotin. The filtrate, or supernatant from the zinc sulfate precipitation, was assayed for radioactivity in a liquid scintillation counter (LS-7000, Beckman, Fullerton, CA). The free biotin at each time point ($x$), the total amount of ligand before the addition of protein ($x_t$), and the amount of free ligand in the presence of protein just prior to the addition of the cold biotin ($x_0$, always less than 6% of $x_t$) were used to calculate the fraction of biotin bound at each time point: $(x_t - x)/(x_t - x_0)$. The dissociation rate constant for the dissociation of the protein−ligand complex ($k_{off}$) was determined from the slope of the line fit to the plot of ln(fraction biotin bound) versus time according to the integrated expression for a first-order reaction rate:

$$\ln\left[\frac{(x_t - x)}{(x_t - x_0)}\right] = \ln(\text{fraction bound}) = -k_{off}t \quad (2)$$

The errors in the dissociation rate constant ($k_{off}$) were calculated from propagation of the errors determined by $\chi^2$ minimization (Igor Pro, Wavemetrics, Inc., Lake Oswego, OR) of the set of two parametrized, linear equations derived from eq 2 in order to incorporate the errors in the time measurements (the independent variable) as well as the errors in the ln(fraction biotin bound) term (the dependent variable).

*Activation Thermodynamic Parameters.* The dissociation kinetics of the biotin−protein complex, for wild-type and the five hydrogen bond mutants, were determined as described above for temperatures ranging from 4 to 37 °C. The activation thermodynamic parameters, $\Delta G^‡$, $\Delta H^‡$, and $\Delta S^‡$ were determined by transition-state analysis of the dependence of the dissociation rate upon temperature, which is described by the Eyring equation (*26*, *27*):

$$k_{off} = \frac{k_B T}{h}\exp\left[\frac{-\Delta G^‡}{RT}\right] \quad (3)$$

$$\Delta G^‡ = \Delta H^‡ - T\Delta S^‡ \quad (4)$$

$$\ln\left[\frac{k_{off}}{T}\right] = -\frac{\Delta H^‡}{RT} + \left[\frac{\Delta S^‡}{R} + \ln\left(\frac{k_B}{h}\right)\right] \quad (5)$$

where $k_B$ is the Boltzmann constant, $h$ is Planck's constant, and $R$ is the molar gas constant. The slope and intercept of the line fit to the plot of $\ln(k_{off}/T)$ versus $1/T$ yield $\Delta H^‡$, and $\Delta S^‡$, respectively. The errors in the activation thermodynamic parameters were calculated from the propagation of the errors determined by $\chi^2$ minimization (Igor Pro, Wavemetrics, Inc., Lake Oswego, OR) of the set of two parametrized, linear equations derived from eq 5 in order to incorporate the errors in the temperature measurements, as well as the errors in the $\ln(k_{off}/T)$ term.

## RESULTS

*Equilibrium Alterations.* A new competitive binding assay for determining the relative equilibrium free energies of mutants relative to wild-type streptavidin was developed. The competition curves at 37 °C (where the reduced dissociation half-life allows thermodynamic equilibration) generated for each of the hydrogen bond mutants are displayed in Figure 2. Each solid curve represents the fit of the solution of eq 1 to the data using the ratio of the streptavidin−biotin equilibrium dissociation constants ($\Delta K_d$) as the fitting parameter. The control experiment with wild-type streptavidin competing with the wild-type-HisTag for [$^3$H]biotin yielded a ratio of equilibrium constants of 0.96, which is

Table 1: Summary of Kinetic and Equilibrium Characterization of Hydrogen-Bonding Mutants at 37 °C, Except Where Noted

| protein | $k_{off}$ ($s^{-1}$) × $10^{-5}$ | $\Delta k_{off}$[a] | $\Delta K_d$[b] | $\Delta\Delta G°$ [c] (kcal/mol) | $\Delta H°$ (kcal/mol) | $\Delta H°$ (25 °C) (kcal/mol) |
|---|---|---|---|---|---|---|
| WT | 4.3 ± 0.2 | | 0.96 ± 0.04 (0.85, 1.07) | | −29.4 | −24.9 ± 0.4 |
| Y43F | 20 ± 1 | 4.9 | 6.9 ± 0.2 (6.3, 7.6) | 1.2 | −28.2 | −27.5 ± 0.9 |
| Y43A | 380 ± 60 | 93 | 67 ± 3 (61, 74) | 2.6 | −21.6 | −16. ± 1.4 |
| S27A | 660 ± 40[d] | 161 | 114 ± 3 (106, 123) | 2.9 | −24.5 | −23.3 ± 0.6 |
| N23E | 770 ± 60 | 188 | 69 ± 3 (63, 75) | 2.6 | −25.7 | −24.0 ± 1.0 |
| N23A | 1030 ± 220 | 251 | 282 ± 9 (259, 308) | 3.5 | −21.5 | −18.0 ± 0.6 |

[a] $\Delta k_{off} = k_{off}$(mutant)/$k_{off}$(WT). [b] $\Delta K_d = K_d$(mutant)/$K_d$(WT). The standard deviations are estimated from the propagation of errors in measurements. The parameter values determined at the 99% confidence intervals are given in parentheses. [c] $\Delta\Delta G° = \Delta G°$(mutant) − $\Delta G°$(WT) = $RT$ ln $\Delta K_d$. Characterization was performed at 37 °C. [d] Kinetic data for S27A at 37 °C was calculated from the transition-state plot, with the standard deviation computed from the errors in the transition-state slope and intercept.

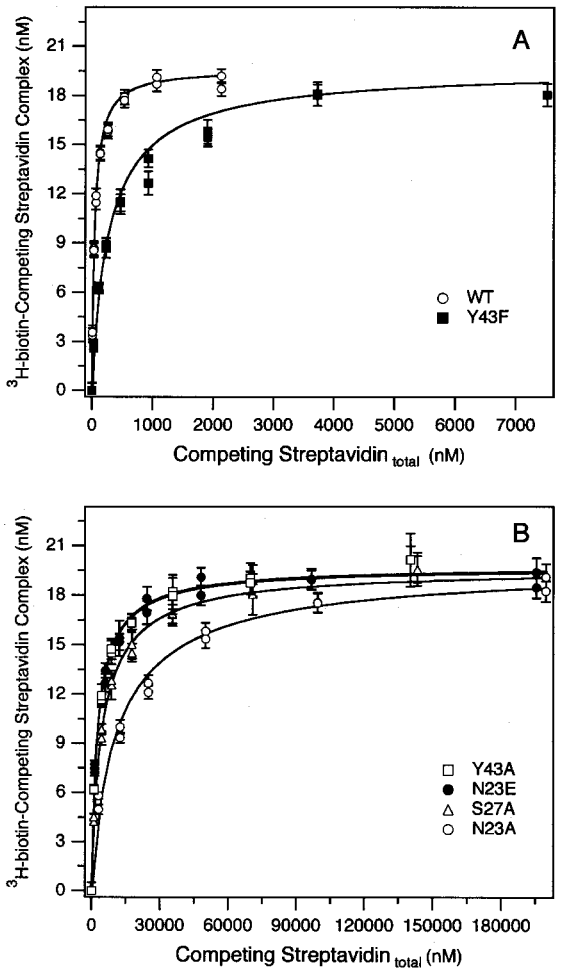


FIGURE 2: Competition curves at 37 °C for streptavidin variants competing with WT-HisTag protein for [$^3$H]biotin. (a) WT streptavidin (open circle) and Y43F (solid square); (b) S27A (open triangle), Y43A (open square), N23E (solid circle), and N23A (open circle). The curves are the fit of the solution of eq 1 to the data with $\Delta K_d$ as the fitting parameter.

within experimental error of the expected ratio of 1.0. Table 1 summarizes the ratio of the equilibrium dissociation constants ($\Delta K_d$) and $\Delta\Delta G°$ values determined at 37 °C. All of the mutants display relatively large free-energy alterations. The Y43F mutation reduced the binding free energy by 1.2 kcal/mol, the Y43A and N23E by 2.6 kcal/mol, S27A by 2.9 kcal/mol, and N23A by 3.5 kcal/mol. The summary of the isothermal titrating calorimetry results at 25 °C and 37 °C are also reported in Table 1. The Y43A and N23A mutants display large decreases in binding enthalpy at 25 °C with $\Delta\Delta H°$ of 8.9 and 6.9 kcal/mol, respectively. The N23E mutant displays a small decrease in $\Delta H°$ that is within experimental error of wild-type, and S27A also displays a relatively small $\Delta\Delta H°$ of 1.6 kcal/mol. The change in equilibrium-binding enthalpy for Y43F favors association over WT at 25 °C ($\Delta\Delta H° = -2.6$ kcal/mol), demonstrating that the ground-state free-energy destabilization is entropically driven. The binding enthalpies were also measured at 37 °C where the $\Delta\Delta G°$ values could be determined, allowing a dissection of the enthalpic and entropic components of the free-energy alterations. For all of the mutants except Y43F, the free-energy alterations arise from large enthalpic and entropic components that partially cancel each other. These preliminary two temperature point results also suggest that the Y43A and N23A mutations result in large alterations in $\Delta C_p°$, although precise determinations await measurements over a full temperature range.

*Dissociation Kinetics and Activation Parameters.* The dissociation kinetics for the WT and the mutants were monoexponential and first order for all of the temperatures studied, with the 25 °C data shown in Figure 3. The rate constants ($k_{off}$) at 37 °C were determined from the slopes of the dissociation plots at 37 °C (data not shown) and are summarized in Table 1. The conservative Y43F mutation resulted in a small increase in $k_{off}$ (4.9-fold), while mutation to alanine resulted in a 93-fold increase in $k_{off}$. The S27A, N23A, and N23E mutants displayed large increases in $k_{off}$ with alterations of 161-, 188-, and 251-fold, respectively. The energetics of the activation barrier to dissociation were determined by applying transition-state theory to the measured temperature dependence of the dissociation rates. The Eyring plots of ln($k_{off}/T$) versus $1/T$ shown in Figure 4 were linear for all of the streptavidin mutants over the temperature range used here. Table 2 summarizes the activation thermodynamic parameters calculated from the least-squares fit of the data in Figure 4 to eq 5. This model assumed a single averaged transition state. Y43F has a slightly higher enthalpic barrier (by +0.8 kcal/mol) but a more positive activation entropy (by +1.9 kcal/mol) than wild-type, resulting in a net lowering of the total barrier by 1.1 kcal/mol. The enthalpic barriers for Y43A, N23E, and N23A are

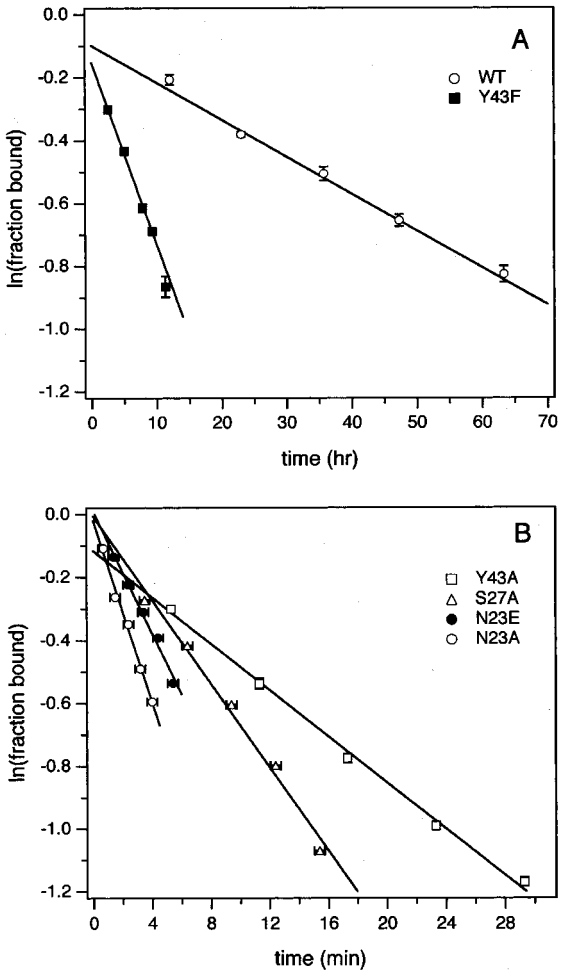


FIGURE 3: Streptavidin−biotin dissociation rate at 25 °C. (a) WT streptavidin (open circle) and Y43F (solid square); (b) Y43A (open square), S27A (open triangle), N23E (solid circle), and N23A (open circle).

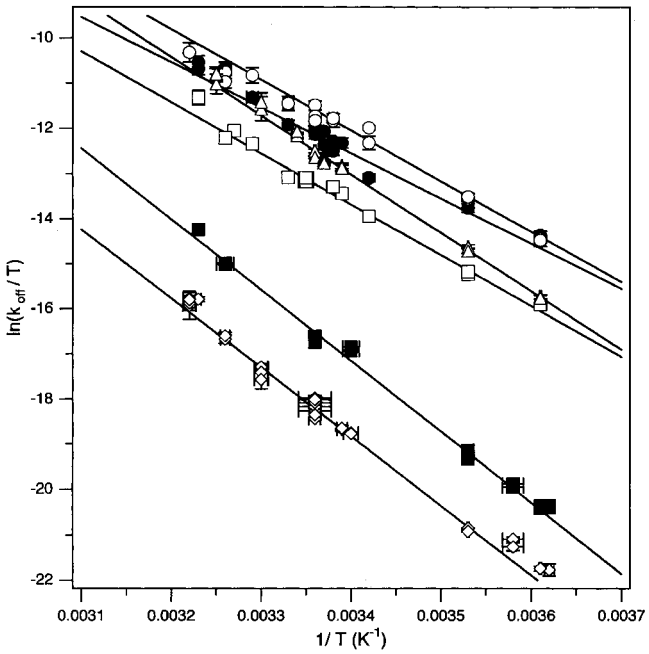


FIGURE 4: Eyring plots for the dissociation of the streptavidin−biotin complex. Lines are fits of Eyring transition state theory (eq 5) for WT (open diamond), Y43F (solid square), Y43A (open square), S27A (open triangle), N23E (solid circle), and N23A (open circle).

Table 2: Activation Thermodynamic Parameters for the Dissociation Reaction (kcal/mol)

| protein | $\Delta H^{\ddagger}$ | $T\Delta S^{\ddagger}$ (37 °C) | $\Delta G^{\ddagger}$ (37 °C) |
|---|---|---|---|
| WT | 30.4 ± 0.2 | 5.8 ± 0.1 | 24.6 ± 0.3 |
| Y43F | 31.2 ± 0.3 | 7.7 ± 0.2 | 23.5 ± 0.3 |
| Y43A | 22.4 ± 0.5 | 0.6 ± 0.5 | 21.8 ± 0.7 |
| S27A | 25.8 ± 0.3 | 4.5 ± 0.3 | 21.3 ± 0.4 |
| N23E | 20.0 ± 0.5 | −1.3 ± 0.5 | 21.3 ± 0.6 |
| N23A | 22.3 ± 0.4 | 1.4 ± 0.4 | 20.9 ± 0.6 |

lowered from the wild-type value, while their activation entropies are significantly less positive (the N23E activation entropy becomes negative and unfavorable). The S27A kinetic alterations are nearly entirely enthalpic in origin with a relatively small change in activation entropy.

## DISCUSSION

The initial site-directed mutagenesis studies of the residues directly hydrogen bonded to the ureido oxygen of biotin suggest that these interactions are indeed relatively strong compared to those observed in other protein−ligand systems. The values of $\Delta\Delta G°$ obtained for the S27A and N23A mutants at 2.9 and 3.5 kcal/mol are more in line with those typically observed for mutating hydrogen-bonding side chains with one charged partner (*28*). These findings are consistent with Weber's hypothesis that the ureido oxygen exists as an oxyanion in the bound state (*24*). The Y43F alteration at 1.2 kcal/mol is on the upper border of typical values for two neutral partners (*28*). Fersht and others have pointed out that most hydrogen-bonding residues are likely to be bonded to water in the ligand-free state, so that the $\Delta\Delta G°$ values measured upon mutagenesis are often smaller than predicted because they represent the differential binding energy between water and ligand. In addition, $\Delta\Delta G°$ values measured by protein engineering can also include cooperative effects, van der Waals interactions introduced with the new side chain, configurational entropy, etc. The values thus measured in protein engineering experiments cannot be considered to be intrinsic hydrogen-bonding free energies. The large reductions in binding free energy are consistent with cooperative effects, which can be expected with streptavidin due to the presence of the hydrogen-bonding network. It is also possible that water presence and structure is altered in the mutants, and further interpretation awaits the determination of the mutant structures in the bound and unbound states.

There is a wide but often controversial body of literature on hydrogen-bonding thermodynamics from model and protein studies (ref *29* provides a review of fundamental literature; *30*). Most studies have concentrated on the equilibrium parameters, where the intrinsic enthalpy of hydrogen bond formation in water is favorable and the entropy is generally considered to be unfavorable, although Williams has postulated that in some cases the release of hydrogen-bonded water from amides upon amide−amide hydrogen bond formation can also give rise to a favorable entropy term (*31*). The mutation of Tyr 43 to Phe in streptavidin results in a more negative-binding enthalpy at 25 °C and an overall small decrease in the binding free energy. A similar result has been reported by Connelly and co-workers in the FK506 interaction with tacrolimus and

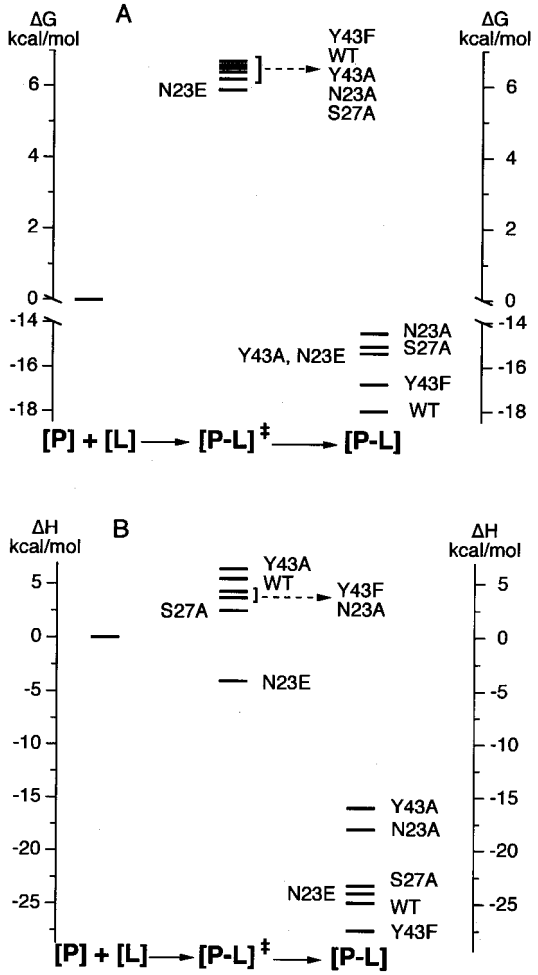


FIGURE 5: Thermodynamic profiles for the streptavidin−biotin dissociation reaction coordinate evaluated for WT, S27A, N23A, N23E, Y43A, and Y43F. (a) Gibbs free energy at 37 °C and (b) enthalpy at 37 °C.

rapamycin (*32*). Their thermodynamic analysis suggested that the enthalpies associated with breaking tyrosine−water and water−water hydrogen bonds dominated the breaking of tyrosine−ligand hydrogen bonds. They also observed that the overall binding free energy was decreased upon mutation of Tyr to Phe because of an unfavorable entropy term, which was interpreted as a decrease in entropy associated with water release from the phenyl side chain upon ligand binding. The determination of the Y43F bound streptavidin structure should clarify whether a similar mechanism is responsible for our results. Chemical modification of the corresponding tyrosine in the closely related avidin protein has been previously shown to strongly modulate the affinity for biotin (*33*), although the mutagenesis results here suggest that removal of the Tyr 43 hydrogen bond does not result in a particularly large free-energy alteration.

The dissociation reaction coordinate is a particularly important aspect of high-affinity interactions, as it is the activation barrier to dissociation that typically separates high- from low-affinity interactions (*25*, *34*−*36*). The streptavidin−biotin binding equilibrium and activation barrier are both enthalpically driven. The free-energy and enthalpy profiles of the dissociation reaction coordinate for WT streptavidin and the hydrogen-bonding mutants are shown in Figure 5. The magnitude of the $\Delta K_d$ was similar in magnitude to the $\Delta k_{off}$ for all mutants except N23E. Therefore, the decrease in the biotin affinity from the wild-type affinity for the conservative Y43F, S27A, and N23A mutants (and also for Y43A) reflects a free-energy destabilization of the ligand-bound state for these mutants. In the context of a single transition-state model, this would suggest that the ureido oxygen hydrogen-bonding interactions are broken in the transition state. The alteration of each ureido oxygen hydrogen-bonding position lowers the enthalpic barrier to dissociation in all but one case, thereby reducing the total activation ($\Delta G^{\ddagger}$) barrier. For Y43F, the enthalpic contribution to the activation barrier is increased over that of wild-type, with a more positive and favorable activation entropy. For N23E, the $\Delta k_{off}$ was greater than the $\Delta K_d$ suggesting that there is a free-energy destabilization of the transition state in addition to the free-energy destabilization of the ligand-bound ground state.

In summary, the conservative mutations of hydrogen-bonding interactions at the ureido oxygen of biotin result in relatively large alterations in the free energy of ligand association. While these changes likely reflect cooperative network effects, they strongly suggest that the ureido binding pocket indeed contributes an unusually large free energy for uncharged hydrogen-bonding interactions. The transition-state mapping also suggests that the ureido oxygen interactions are broken by the transition state, as conservative mutations result largely in ground-state destabilization and relatively small alterations in the transition-state energies. Further mutagenesis studies with double mutant cycles at the ureido oxygen-binding pocket and at the biotin nitrogen and sulfur positions should provide further insight into the hydrogen-bonding energetic contributions in this system.

## ACKNOWLEDGMENT

We thank Saurabh Gupta for the construction of the S27A, Ashutosh Chilkoti for the construction of the Y43F gene, and Professor Michael Gelb for helpful suggestions on the competitive binding experiments.

## REFERENCES

1. Freitag, S., LeTrong, I., Klumb, L., Stayton, P., and Stenkamp, R. E. (1997) *Protein Sci. 6*, 1157−1166.
2. Hendrickson, W. A., Pahler, A., Smith, J. L., Satow, Y., Merritt, E. A., and Phizackerley, R. P. (1989) *Proc. Natl. Acad. Sci. U.S.A. 86*, 2190−2194.
3. Livnah, O., Bayer, E. A., Wilchek, M., and Sussman, J. L. (1993) *Proc. Natl. Acad. Sci. U.S.A. 90*, 5076−5080.
4. Pugliese, L., Coda, A., Malcovati, M., and Bolognesi, M. (1993) *J. Mol. Biol. 231*, 698−710.
5. Weber, P. C., Ohlendorf, D. H., Wendoloski, J. J., and Salemme, F. R. (1989) *Science 243*, 85−88.
6. Bibbins, K. B., Boeuf, H., and Varmus, H. E. (1993) *Mol. Cell. Biol. 13*, 7278−7287.
7. Hibbits, K. A., Gill, D. S., and Willson, R. C. (1994) *Biochemistry 33*, 3584−3590.
8. Kelley, R. F., Costas, K. E., O'Connell, M. P., and Lazarus, R. A. (1995) *Biochemistry 34*, 10383−10392.
9. Middleton, S. A., Johnson, D. L., Jin, R., McMahon, F. J., Collins, A., Tullai, J., Groninger, R. H., Jolliffe, L. K., and Mulcahy, L. S. (1996) *J. Biol. Chem. 271*, 14045−14054.
10. Sudol, M., Chen, H. I., Bougeret, C., Einbond, A., and Bork, P. (1995) *FEBS Lett. 369*, 67−71.
11. Basran, J., Casarotto, M. G., Barsukov, I. L., and Roberts, G. C. K. (1995) *Biochemistry 34*, 2872−2882.
12. Carlow, D. C., Smith, A. A., Yang, C. C., Short, S. A., and Wolfenden, R. (1995) *Biochemistry 34*, 4220−4224.

13. Hayashi, H., Inoue, K., Mizuguchi, H., and Kagamiyama, H. (1996) *Biochemistry 35*, 6754−6761.
14. Krebs, J. F., Ippolito, J. A., Christianson, D. W., and Fierke, C. A. (1993) *J. Biol. Chem. 268*, 27458−27466.
15. Tsumoto, K., Ueda, Y., Maenaka, K., Watanabe, K., Ogasahara, K., Yutani, K., and Kumagai, I. (1994) *J. Biol. Chem. 269*, 28777−29782.
16. Yano, T., Mizuno, T., and Kagamiyama, H. (1993) *Biochemistry 32*, 1810−1815.
17. Falzone, C. J., Wright, P. E., and Benkovic, S. J. (1994) *Biochemistry 33*, 439−442.
18. Kempner, E. S. (1993) *FEBS Lett. 326*, 4−10.
19. Sampson, N. S., and Knowles, J. R. (1992) *Biochemistry 31*, 8482−8487.
20. Chilkoti, A., Tan, P. H., and Stayton, P. S. (1995) *Proc. Natl. Acad. Sci. U.S.A. 92*, 1754−1758.
21. Chilkoti, A., and Stayton, P. S. (1995) *J. Am. Chem. Soc. 117*, 10622−10628.
22. Miyamoto, S., and Kollman, P. A. (1993) *Proteins: Struct., Funct., Genet. 16*, 226−245.
23. Green, N. M. (1962) *Biochim. Biophys. Acta 59*, 244−246.
24. Weber, P. C., Wendoloski, J. J., Pantoliano, M. W., and Salemme, F. R. (1992) *J. Am. Chem. Soc. 114*, 3197−3200.
25. Green, N. M. (1963) *Biochem. J. 89*, 585−591.
26. Eyring, H. J. (1935) *J. Chem. Phys. 3*, 107−115.
27. Evans, M. G., and Polanyi, M. (1935) *Trans. Faraday Soc. 31*, 875−894.
28. Fersht, A. R., Shi, J.-P., Jack, K.-J., Lowe, D. M., and Wilkinson, A. J. (1985) *Nature 314*, 235−238.
29. Rose, G. D. and Wolfenden, R. (1993) *Annu. Rev. Biophys. Bimol. Struct. 22*, 381−415.
30. Habermann, S. M. and Murphy, K. P. (1996) *Protein Sci. 5*, 1229−1239.
31. Doig, A. J., and Williams, D. H. (1992) *J. Am. Chem. Soc. 114*, 338−343.
32. Connelly, P. R., Aldape, R. A., Bruzzese, F. J., Chambers, S. P., Fitzgibbon, M. J., Fleming, M. A., Itoh, S., Livingston, D. J., Navia, M. A., Thomson, J. A., and Wilson, K. P. (1994) *Proc. Natl. Acad. Sci. U.S.A. 91*, 1964−1968.
33. Morag, E., Bayer, E. A., and Wilchek, M. (1996) *Biochem. J. 316*, 193−199.
34. Marchaj, A., Jacobsen, D. W., Savon, S. R., and Brown, K. L. (1995) *J. Am. Chem. Soc. 117*, 11640−11646.
35. Morelock, M. M., Pargellis, C. A., Graham, E. T., Lamarre, D., and Jung, G. (1995) *J. Med. Chem. 38*, 1751−1761.
36. Xu, Y., Nenortas, E., and Beckett, D. (1995) *Biochemistry 34*, 16624−16631.

BI9803123